Protein tyrosine phosphatase 1B inhibition improves endoplasmic reticulum stress-impaired endothelial cell angiogenic response: A critical role for cell survival

SHAHENDA S. ABDELSALAM[1,2], MAZHAR PASHA[1,2], HEBA EL-GAMAL[1,2], MARAM HASAN[1,2], MOHAMED A. ELRAYESS[3], ASAD ZEIDAN[2,4], HESHAM M. KORASHY[1,2] and ABDELALI AGOUNI[1,2,5]

[1]Department of Pharmaceutical Sciences, College of Pharmacy, QU Health; [2]Biomedical and Pharmaceutical Research Unit, QU Health; [3]Biomedical Research Center; [4]Department of Basic Medical Science, College of Medicine, QU Health; [5]Office of Vice President for Research and Graduate Studies, Qatar University, P.O. Box 2713 Doha, Qatar

Received April 3, 2021; Accepted June 28, 2021

DOI: 10.3892/mmr.2021.12304

Abstract. Endoplasmic reticulum (ER) stress contributes to endothelial dysfunction, which is the initial step in atherogenesis. Blockade of protein tyrosine phosphatase (PTP)1B, a negative regulator of insulin receptors that is critically located on the surface of ER membrane, has been found to improve endothelial dysfunction. However, the role of ER stress and its related apoptotic sub-pathways in PTP1B-mediated endothelial dysfunction, particularly its angiogenic capacity, have not yet been fully elucidated. Thus, the present study aimed to investigate the impact of PTP1B suppression on ER stress-mediated impaired angiogenesis and examined the contribution of apoptotic signals in this process. Endothelial cells were exposed to pharmacological ER stressors, including thapsigargin (TG) or 1,4-dithiothreitol (DTT), in the presence or absence of a PTP1B inhibitor or small interfering (si)RNA duplexes. Then, ER stress, angiogenic capacity, cell cycle, apoptosis and the activation of key apoptotic signals were assessed. It was identified that the inhibition of PTP1B prevented ER stress caused by DTT and TG. Moreover, ER stress induction impaired the activation of endothelial nitric oxide synthase (eNOS) and the angiogenic capacity of endothelial cells, while PTP1B inhibition exerted a protective effect. The results demonstrated that blockade or knockdown of PTP1B prevented ER stress-induced apoptosis and cell cycle arrest. This effect was associated with reduced expression levels of caspase-12 and poly (ADP-Ribose) polymerase 1. PTP1B blockade also suppressed autophagy activated by TG. The current data support the critical role of PTP1B in ER stress-mediated endothelial dysfunction, characterized by reduced angiogenic capacity, with an underlying mechanism involving reduced eNOS activation and cell survival. These findings provide evidence of the therapeutic potential of targeting PTP1B in cardiovascular ischemic conditions.

Correspondence to: Dr Abdelali Agouni, Department of Pharmaceutical Sciences, College of Pharmacy, QU Health, Qatar University, Building I06, P.O. Box 2713 Doha, Qatar
E-mail: aagouni@qu.edu.qa

Key words: protein tyrosine phosphatase 1B, tyrosine phosphatases, endoplasmic reticulum stress, endothelial dysfunction, angiogenesis, apoptosis

Introduction

Endothelial dysfunction is a state in which the endothelial layer of vessels undergoes structural changes and functional impairment, which is characterized by reduced nitric oxide (NO) synthesis, impairment of endothelial-mediated vasodilation and dysregulated angiogenesis (1). Endothelial dysfunction is considered as an independent predictor of perturbations in the cardiovascular system and is the initial step in the progression of cardiovascular diseases. This is due to its central role in the commencement of atherosclerotic events and the progression of clinical cardiovascular complications associated with several conditions, such as diabetes and hypertension (2). Several factors affect endothelial function, including insulin due to its ability to enhance the bioavailability of endothelium-derived NO via its interaction with vascular endothelial cell insulin receptors (3). Binding of insulin results in the auto-phosphorylation of the receptor and subsequent downstream activation of the PI3K/Akt signaling pathway, thereby activating the key enzyme responsible for NO synthesis, endothelial NO synthase (eNOS) (4,5). It has been shown that conditions characterized by insulin resistance, such as diabetes and obesity, are closely associated with endothelial dysfunction (3).

Protein tyrosine phosphatase (PTP) 1B is a soluble non-transmembrane and cytosolic tyrosine-specific phosphatase that has been implicated in several pathological conditions, including diabetes and obesity (6,7). Due to its tyrosine phosphatase activity, PTP1B negatively regulates the insulin receptor, thus serving a critical role in insulin resistance (8). Accumulating evidence has suggested that PTP1B attenuates insulin signaling, and hence, may impair the vascular effects mediated by insulin (9). PTP1B has also been shown to contribute to endothelial dysfunction and

cardiovascular disorders (9). Several models of PTP1B genetic deletion and pharmacological inhibition have been used to assess this role of PTP1B. The inhibition of PTP1B has been reported to be beneficial in restoring endothelial function and NO-mediated vasodilation in a mouse model chronic heart failure (CHF) (10). Furthermore, deletion of PTP1B was found to protect the mice against CHF-induced (11) and high fat diet-induced endothelial dysfunction (12). In these models, endothelial function was preserved, and was accompanied by an increase in eNOS phosphorylation. In adult mice, the selective deletion of PTP1B in endothelial cells resulted in an improvement in mouse survival, cardiac function and cardiac hypertrophy (13). Moreover, endothelial PTP1B-deficient mice exhibited an improvement in vascular angiogenic capacity, increased VEGFR phosphorylation, upregulation of eNOS expression and a substantial decline in the development of cardiac fibrosis (13). Although the deletion and inhibition of PTP1B has been proven to be beneficial for both whole-body glucose homeostasis and endothelial function, the molecular mechanisms via which PTP1B negatively alters endothelial functions are not yet fully understood.

PTP1B has been reported to serve a role in the activation of the endoplasmic reticulum (ER) stress response (14,15), which is an inflammatory pathway that has emerged as a strong molecular link between insulin resistance and endothelial dysfunction (1,16,17). The ER stress response is triggered in obesity and can cause insulin resistance and lipid accumulation (18-20), as well as serve a crucial role in cardiovascular dysfunction (21,22). The ER is the site for protein synthesis and folding, and the synthesis of lipids and steroids, as well as being a large store for intracellular calcium (17). The ER ensures that proteins are properly folded and prevents their aggregation (23,24). Physiological and pathological disturbances can overwhelm the ER due to the surge in protein demand, resulting in the build-up of misfolded proteins within the lumen of the ER. This activates an adaptive mechanism known as the unfolded protein response (UPR), which aims to restore ER homeostasis and increase ER folding capacity (17,23,25-28). The UPR mediates its actions via three major ER transmembrane sensors: Inositol requiring enzyme-1α, activating transcription factor (ATF)-6 and protein kinase-like ER kinase, which become activated upon dissociating from the ER resident chaperone immunoglobulin binding protein (BiP), also known as heat shock protein family A (Hsp70) member 5 (HSPA5), in response to the accumulation of unfolded proteins within the ER (17,23,25-28). However, the sustained activation of the UPR due to continued stress results in a switch from the adaptive UPR to the pro-apoptotic and pro-inflammatory ER stress response, causing cell inflammation, dysfunction and ultimately cell death (17,23,25-28).

Previous studies have shown that ER stress activation is responsible for endothelial cell apoptosis and decreased eNOS expression (1,17,29). Moreover, in mice treated with angiotensin-II, endothelial function was found to be preserved when ER stress was inhibited, as evidenced by an enhancement in eNOS activity and phosphorylation levels, as well as the amelioration of endothelial-mediated vasodilation (21). The pharmacological induction of ER stress has been observed to reduce angiogenic capacity via a mechanism involving reactive oxygen species and cell death in human umbilical vein endothelial cells (HUVECs) (30). Activation of ER stress can increase endothelial cell apoptosis via the elevated expression level of the pro-apoptotic factor CHOP and enhanced JNK phosphorylation (31).

PTP1B has been shown play a role in activating the ER stress response in a complex interaction with insulin resistance in mouse models of obesity, due to its critical location at the surface of ER membrane. For instance, it has been demonstrated that liver-PTP1B deletion from birth or induced in adult mice can decrease obesity-stimulated ER stress in mouse livers (14,15). By inducing the ER stress response, PTP1B overactivation may lead to endothelial cell death, promotion of a prothrombotic state and endothelial dysfunction (32). However, to the best of our knowledge, the role of ER stress and its related key apoptotic signals in PTP1B-mediated endothelial dysfunction, particularly in relation to its angiogenic capacity, have not yet been investigated. Therefore, the aim of the present study was to examine the impact of PTP1B suppression on ER stress-mediated endothelial cell dysfunction and impaired angiogenic response, and to assess the contribution of ER stress-induced apoptosis and activation of underlying apoptotic pathways in this process.

Materials and methods

Cell culture. EA.hy926 [ATCC® CRL-2922™; American Type Culture Collection (ATCC)] endothelial cells were cultured in DMEM containing high glucose and 10% FBS, supplemented with 1% penicillin/streptomycin (P/S), sodium pyruvate (1%) and L-glutamine (1%) (all from Gibco; Thermo Fisher Scientific, Inc.). Cells were incubated at 37˚C with 5% CO_2 and 95% humidity. Cells were only cultured up to passage 20 in these experiments.

To culture primary HUVECs (ATCC® PCS-100-010™; ATCC), cells were maintained in medium 200 containing low serum growth supplement (2%) and supplemented with P/S (1%) (all from Gibco; Thermo Fisher Scientific, Inc.). Cells were placed inside an incubator at 37˚C with 5% CO_2 and 95% humidity. HUVECs used in experiments were between passage 1 and 6. Based on the regulations of the Ministry of Public Health in Qatar, the Institutional Review Board (IRB) of Qatar University (Doha, Qatar) has categorized the use of these commercially sourced and de-identified HUVECs as non-human subject research and hence exempted the study from IRB ethics review (QU-IRB 008-NR/21).

Cell treatments. For all treatments, 6-well plates were seeded with endothelial cells (200,000 cells/well) prior to treatment and cultured for 24 h to allow the cells to adhere. ER stress was pharmacologically induced by incubating EA.hy926 cells and HUVECs with 2 mM 1,4-dithiothreitol (DTT; Sigma-Aldrich; Merck KGaA) for 24 h, or 300 nM thapsigargin (TG; Thermo Fisher Scientific, Inc.) for 5 h at 37˚C, respectively. DTT is a strong ER stress inducer that inhibits disulfide bond formation, which results in the improper folding of proteins (33). The unfolded proteins then accumulate within the ER lumen, thereby activating the UPR and ER stress response (17). On the other hand, TG induces ER stress via the inhibition of the Ca^{+2}-ATPase pump, which results in Ca^{+2} depletion from the ER stores (34). To determine the role of PTP1B in ER stress

activation, cells were treated with or without a PTP1B inhibitor (BML-267; Abcam), which was administered at 20 μM for 1 h at 37˚C prior to treatment with DTT or TG (35).

In another set of experiments, HUVECs were stimulated with 20 μM bradykinin (Sigma-Aldrich; Merck KGaA) for 45 min at 37˚C (36), following the treatment of cells with TG (300 nM; 5 h). Then, protein expression and phosphorylation of eNOS was assessed via western blotting. HUVECs were also exposed or not to TG with or without PTP1B inhibitor, and then stimulated with insulin (Sigma-Aldrich; Merck KGaA) (20 nM; 5 min at 37˚C). Then, protein expression and phosphorylation of Akt was assessed via western blotting.

PTP1B (cat. no. hs.Ri.PTPN1.13.3) (https://eu.idtdna.com/site/order/designtool/index/DSIRNA_PREDESIGN) and control (cat. no. 51-01-19-08) (https://eu.idtdna.com/site/order/stock/index/trifecta) small interfering (si) RNA duplexes were designed and synthesized by Integrated DNA Technologies, Inc., and were used for all PTP1B gene silencing experiments. Briefly, 50,000 HUVECs/well were seeded into 6-well plates, followed by a 24-h incubation to allow the cells to adhere. According to the manufacturer's protocol, cells were transfected the following day with either control or PTP1B siRNA duplexes (15 nM) using INTERFERin® transfection reagent (Polyplus-transfection SA). Negative control cells were left untreated. Cells were incubated for 24 h, after which the medium was replaced with fresh complete medium. Cells were treated for a total duration of 48 h, prior to treatment with 300 nM TG for 5 h. Western blot analysis showed that protein expression level of PTP1B was not affected when cells were treated with scrambled control siRNA duplexes (data not shown), and therefore, the remainder of experiments were conducted using 'untreated cells' as negative controls.

Western blot analysis. Following cell treatments, the medium was aspirated and discarded, and then cells were washed with ice-cold PBS (Thermo Fisher Scientific, Inc.). Next, EA.hy926 cells or HUVECs were lysed in cold RIPA lysis buffer (Tris (0.5 M, pH 6.8) and SDS (20%); Thermo Fisher Scientific, Inc.) supplemented with a cocktail of protease and phosphatase inhibitors (Thermo Fisher Scientific, Inc.). The protein concentration was determined using a BCA assay (Thermo Fisher Scientific, Inc.). Equal quantities of proteins (10-20 μg) were separated using SDS-PAGE gels (8-12%, according to the molecular weights of targets). Proteins were then transferred to PVDF membranes (Thermo Fisher Scientific, Inc.), which were blocked for 1 h at room temperature in TBS containing 0.1% Tween-20 (TBST; Sigma-Aldrich; Merck KGaA) and either 5% BSA (Thermo Fisher Scientific, Inc.) (phosphorylated targets) or dry milk. Membranes were then washed with TBST and incubated with the following primary antibodies overnight at 4˚C: BiP (cat. no. 3183S), CHOP (cat. no. 2895S), phosphorylated (p)-eNOS (Ser1177; cat. no. 9571S), eNOS (cat. no. 5880S), p-Akt (Ser473; cat. no. 4060L), Akt (cat. no. 4691L), cleaved caspase-9 (cat. no. 9505S), cleaved poly (ADP-ribose) polymerase (PARP-1; cat. no. 5625S), p-ERK 1/2 MAPK (Thr202/204; cat. no. 9106S), ERK 1/2 MAPK (cat. no. 9102S), LC-3 I/II (cat. no. 12741S), and PTP1B (cat. no. 5311S; all 1:1,000; Cell Signaling Technology, Inc.), caspase-12 (cat. no. ab18766; 1:1,000; Abcam) and mouse anti-β-actin (cat. no. sc-47778; 1:5,000; Santa Cruz Biotechnology, Inc.). Membranes were then washed again with TBST and incubated for 1 h at room temperature with the corresponding HRP-conjugated anti-rabbit (cat. no. 7074S) or anti-mouse (cat. no. 7076S) secondary antibodies (1:10,000; Cell Signaling Technology, Inc.). To visualize the chemiluminescence signal, membranes were incubated with SignalFire™ Elite ECL reagent (Cell Signaling Technology, Inc.) and images were captured using FluorChem™ M imaging system (ProteinSimple). Densitometry was conducted using Scion image software 4.0 (Scion Corporation) to assess protein band intensity.

Total RNA isolation and gene expression analysis using reverse transcription-quantitative (RT-q)PCR. After treatments, EA.hy926 cells or HUVECs were washed, trypsinized and collected. The innuPREP RNA Mini kit (Analytik Jena AG) was used to extract total RNA as per the manufacturer's protocol. A NanoDrop 2000 system (Thermo Fisher Scientific, Inc.) was used to determine the concentration and quality of RNA. For reverse transcription, a RevertAid Reverse Transcription kit (Thermo Fisher Scientific, Inc.) and an oligo (dT) 12-18 primer were used to synthesize cDNA from a total of 500 ng RNA, following the manufacturer's instructions. A mixture of cDNA, human primers for target genes (primer pair sequences are summarized in Table I) and GoTaq® qPCR Master mix (Promega Corporation) were amplified in an Applied Biosystems 7500 Fast Real-Time PCR system (Thermo Fisher Scientific, Inc.) (33). The thermocycling conditions were as follows: holding at 95˚C for 10 min, cycling stage (40 cycles; 95˚C for 15 sec, 60˚C for 60 sec, 72˚C for 40 sec), and holding stage at 95˚C for 60 s, followed by melting curve analysis. Experiments were conducted with six independent biological repeats. To assess relative gene expression, the comparative $2^{-\Delta\Delta Cq}$ method (37) was used to analyze data. mRNA expression was normalized against the housekeeping gene *β-actin* and reported as fold-change after normalization to control group. Sourcing of the human primers pairs was conducted using the PrimerBank (https://pga.mgh.harvard.edu/primerbank/), followed by their synthesis by Sigma-Aldrich (Merck KGaA).

Endothelial cell tube-like structures formation assay. The angiogenic capacity of endothelial cells was assessed *in vitro* using a Geltrex™ Matrigel matrix (Thermo Fisher Scientific, Inc.). HUVECs were seeded into 6-well plates (200,000 cells/well) and left for 24 h to adhere. The following day, cells were treated with 300 nM TG for 5 h with or without 20 μM PTP1B inhibitor at 1 h prior to treatment with TG. Control cells were left untreated. Geltrex™ was stored overnight in the refrigerator (4˚C) for thawing prior to the experiment. On the experiment day, Geltrex™ (100 μl) was loaded onto 24-well plates and the gel was spread uniformly. The gel was allowed to solidify by placing the gel-coated wells in the incubator (37˚C) for 30 min. During the gel incubation time, treated cells were collected and counted. Then, a cell suspension containing 50,000 cells (100 μl) was added onto each well. The plates were placed back inside the incubator. Tube formation was visualized, and images were captured after 4 h of incubation using a phase contrast inverted microscope at x40 magnification (OPTIKA Srl). Web-based WimTube software from Wimasis Image Analysis (Onimagin

Table I. List of human primer pairs used in the present study.

Target gene	Forward primer (5'→3')	Reverse primer (5'→3')
ATF-4	CCCTTCACCTTCTTACAACCTC	TGCCCAGCTCTAAACTAAAGGA
β-actin	CATGTACGTTCGTATCCAGGC	CTCCTTAATGTCACGCACGAT
BiP	CATCACGCCGTCCTATGTCG	CGTCAAAGACCGTGTTCTCG
CHOP	GAACGGCTCAAGCAGGAAATC	TTCACCATTCGGTCAATCAGAG
FGF-1	ACACCGACGGGCTTTTATACG	CCCATTCTTCTTGAGGCCAAC
FGF-2	AGAAGAGCGACCCTCACATCA	CGGTTAGCACACACTCCTTTG
GRP94	GCTGACGATGAAGTTGATGTGG	CATCCGTCCTTGATCCTTCTCTA
ICAM-1	ATGCCCAGACATCTGTGTCC	GGGGTCTCTATGCCCAACAA
IL-6	AAATTCGGTACATCCTCGACGG	GGAAGGTTCAGGTTGTTTTCTGC
IL-8	ACTGAGAGTGATTGAGAGTGGAC	AACCCTCTGCACCCAGTTTTC
MCP-1	TTAAAAACCTGGATCGGAACCAA	GCATTAGCTTCAGATTTACGGGT
PTP1B	GCAGATCGACAAGTCCGGG	GCCACTCTACATGGGAAGTCAC
VEGF-A	AGGGCAGAATCATCACGAAGT	AGGGTCTCGATTGGATGGCA

ATF-4, activating transcription factor 4; BiP, endoplasmic reticulum resident chaperone immunoglobulin binding protein; FGF, fibroblast growth factor; GRP94, 94 kDa glucose-regulated protein; ICAM-1, intracellular molecular adhesion-1; MCP-1, monocyte chemoattractant protein-1; PTP1B, protein tyrosine phosphatase 1B.

Technologies SCA) was used to semi-quantitatively analyze the images. The comparison across the experimental groups was performed by averaging the counted total tube lengths per condition, from five random blind fields.

Tali-based assay for apoptosis and cell cycle analysis. A Tali™ Apoptosis kit (Thermo Fisher Scientific, Inc.) was used, according to the manufacturer's instructions, to assess apoptosis in HUVECs challenged with TG (300 nM; 5 h) with or without PTP1B inhibitor (20 μM) or PTP1B siRNA (15 nM, 48 h). Untreated cells were used as controls. After treatments, cells were collected, washed, and then pelleted via centrifugation at 1,500 x g (5 min; 4˚C). Then, 100 μl 1X Annexin Binding Buffer (ABB) was used to resuspend the pellet. Next, each sample was admixed with 5 μl Annexin V solution and incubated at room temperature for 20 min in the dark. Following the incubation period, samples were centrifuged at 1,500 x g (5 min; 4˚C), and the pellets were resuspended in fresh 1X ABB (100 μl). Finally, samples were mixed with 1 μl PI (100 μg/ml), and the mixture was incubated for 10 min in the dark. Stained cells (25 μl) were loaded into the Tali Cellular Analysis Slides (Thermo Fisher Scientific, Inc.) and imaged using Tali Image-Based Cytometer (Thermo Fisher Scientific, Inc.), following the manufacturer's instructions. The percentages of live, dead and apoptotic cells in each cell preparation were included in the analysis. Representative fluorescence images are presented to indicate apoptotic cells in green color, dead cells in red and green (appear yellow), and live cells with little or no fluorescence.

For cell cycle analysis, cells were harvested following treatments, washed, and then centrifuged at 1,500 x g (5 min; 4˚C). According to the manufacturer's protocol, PI solution (Thermo Fisher Scientific, Inc.) was used to stain the cells. After incubation in the dark for 30 min at 37˚C, stained cells (25 μl) were loaded into the Tali Cellular Analysis Slides (Thermo Fisher Scientific, Inc.) and then imaged using Tali Image-Based Cytometer (Thermo Fisher Scientific, Inc.), according to the manufacturer's instructions. The percentages of cells in each phase of the cell cycle were determined as follows: Sub-G_1 (apoptotic cells), G_0/G_1, S and G_2/M. Representative fluorescence images of cell cycle phases are shown: Red (Sub-G_1), orange (G_0/G_1), blue (S) and green (G_2/M).

Statistical analysis. The data are presented as the mean ± SEM, and 'n' represents the number of biological repeats. The normality of data was tested each time using a Shapiro-Wilk normality test. GraphPad Prism 7.01e software for Mac (GraphPad Software, Inc.) was used to perform the statistical analyses. One-way ANOVA followed by Tukey's multiple comparison post hoc test (for data with Gaussian distribution) or the non-parametric Kruskal-Wallis test followed by Dunn's multiple comparison post hoc test (data with non-Gaussian distribution) were used to analyze the data. $P<0.05$ was considered to indicate a statistically significant difference.

Results

Effect of PTP1B inhibition on ER stress in endothelial cells. The pharmacological induction of ER stress in EA.hy926 cells was achieved by treating cells with DTT (2 mM) for 24 h. Then, the mRNA and protein expression levels of several markers of ER stress were assessed using qPCR and western blot analysis, respectively (Fig. 1). To determine the role of PTP1B in the ER stress response, a group of cells were pre-incubated with a PTP1B inhibitor (20 μM) prior to DTT treatment. It was found that ER stress was significantly induced by DTT, as shown by the significant upregulation in the mRNA expression levels of key ER stress markers, *CHOP* (Fig. 1A), *BiP* (Fig. 1B), 94 kDa glucose-regulated protein (*GRP94*) (Fig. 1C) and *ATF-4* (Fig. 1D). A significant reduction in *CHOP* and

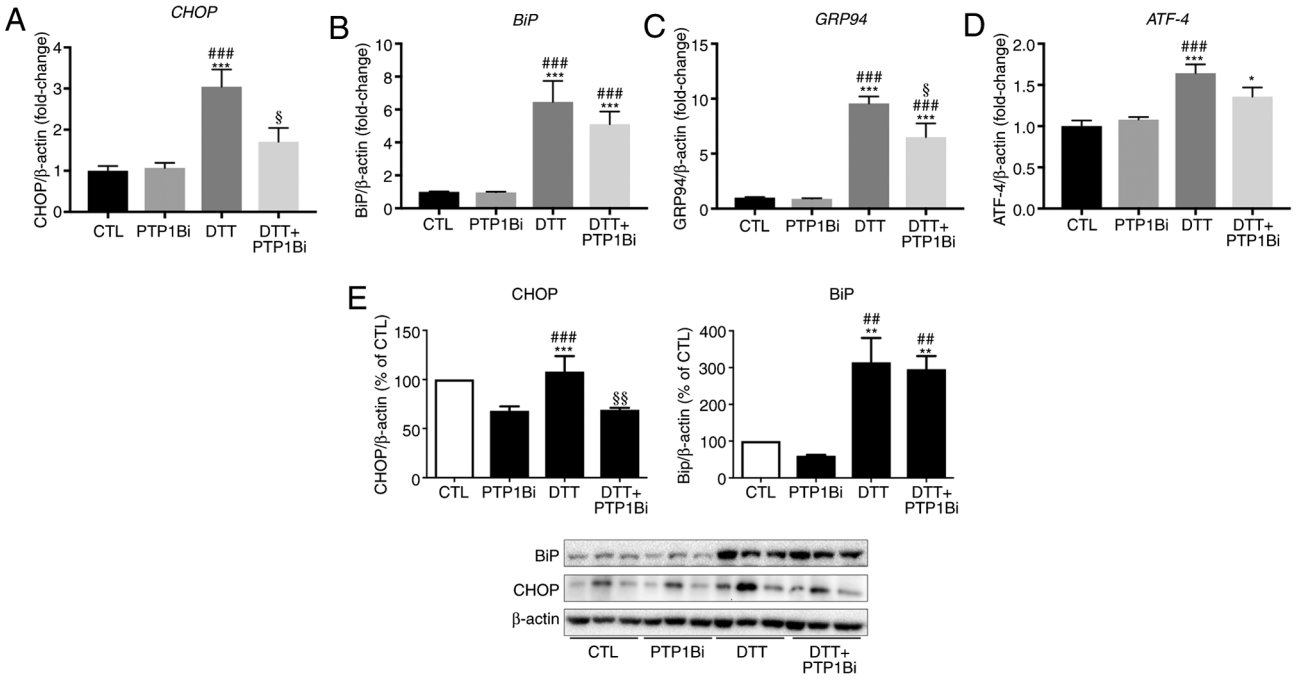

Figure 1. Impact of PTP1B inhibition on pharmacologically-induced endoplasmic reticulum stress in EA.hy926 cells. Reverse transcription-quantitative PCR analysis to assess mRNA expression of (A) *CHOP*, (B) *BiP*, (C) *GRP94* and (D) *ATF-4* and western blot analysis to assess protein expression levels of (E) CHOP and BiP in EA.hy926 endothelial cells exposed to DTT (2 mM, 24 h) with or without PTP1Bi (BML, 20 μM, added 1 h prior to treatment. (A-D) mRNA expression was normalized against the housekeeping gene *β-actin* (n=6 in each group). (E) Bars represent the pooled densitometry data of protein expression of CHOP (left panel) and BiP (right panel) normalized to loading control β-actin and expressed as percentage (%) of untreated group (CTL) (n=4 in each group). All data are presented as the mean ± SEM. *P<0.05, **P<0.01, ***P<0.001 vs. CTL group; $^{\#\#}$P<0.01, $^{\#\#\#}$P<0.001 vs. PTP1Bi group; §P<0.05, §§P<0.01 vs. DTT group. PTP1B, protein tyrosine phosphatase 1B; BiP, endoplasmic reticulum resident chaperone immunoglobulin binding protein; GRP94, 94 kDa glucose-regulated protein; ATF-4, activating transcription factor 4; DTT, 1,4-dithiothreitol; CTL, control; PTP1Bi, PTP1B inhibitor.

GRP94 gene expression was observed after PTP1B inhibition (Fig. 1A and C). Similarly, EA.hy926 cells treated with DTT exhibited an increase in protein expression levels of CHOP and BiP (Fig. 1E). Moreover, PTP1B inhibition caused a significant decrease in protein expression level of CHOP, while the protein expression of BiP was not affected (Fig. 1E left and right panels).

To further validate these results, HUVECs (primary endothelial cells model), were treated with TG (300 nM) for 24 h with or without PTP1B inhibitor. TG treatment resulted in a significant increase in mRNA expression levels of *CHOP* (Fig. 2A), *BiP* (Fig. 2B), *GRP94* (Fig. 2C) and *ATF-4* (Fig. 2D). Furthermore, inhibition of PTP1B significantly prevented the TG-induced effects on all the markers (Fig. 2A-D). Similar to the effects observed with gene expression, after treatment with TG, HUVECs showed a significant enhancement in protein expression levels of CHOP (Fig. 2E, left panel) and BiP (Fig. 2E, right panel). Similarly to EA.hy926 cells, PTP1B inhibition significantly reduced CHOP protein expression, while it had no impact on the protein expression of BiP (Fig. 2E).

Effect of PTP1B inhibition on eNOS and Akt activation in HUVECs subjected to ER stress. The activity of eNOS is a hallmark of endothelial cell function (9,17). To investigate the impact of PTP1B on endothelial function, it is important to assess the effects of PTP1B on the NO signaling pathway. As PTP1B inhibition exerted no changes in the expression level of phosphorylated eNOS (Ser1177) at the basal levels (data not shown), HUVECs were stimulated with bradykinin following the treatment of cells with TG. Bradykinin-treated cells showed a significant increase in eNOS phosphorylation at its activator site (Ser1177) compared to controls (Fig. 3A). However, in cells treated with TG, bradykinin failed to enhance eNOS phosphorylation, and eNOS phosphorylation levels were reduced compared with the untreated control group (Fig. 3A). Of note, the pretreatment of cells with the PTP1B inhibitor significantly prevented the TG-induced effects.

As insulin signaling serves a critical role in the maintenance of endothelial cell function (9), the impact of PTP1B inhibition on the insulin response was assessed. As shown in Fig. 3B, induction of ER stress by TG did not alter insulin-mediated Akt phosphorylation. However, the inhibition of PTP1B enhanced the insulin response, as shown by increased p-Akt expression following insulin treatment (Fig. 3B).

Effect of PTP1B inhibition on the mRNA expression levels of pro-inflammatory genes in endothelial cells subjected to ER stress. ER stress and endothelial dysfunction are closely associated with cellular inflammation (17). Endothelial dysfunction precedes and imitates inflammatory response, where, at their surface, dysfunctional endothelial cells expose various adhesion molecules, such as intracellular molecular adhesion (ICAM)-1, together with the release of multiple pro-inflammatory cytokines and chemokines, including IL-6, IL-8, and monocyte chemoattractant protein (MCP)-1. In this context, PTP1B is involved in the regulation of inflammatory responses (9,38). Therefore, the impact of PTP1B inhibition on

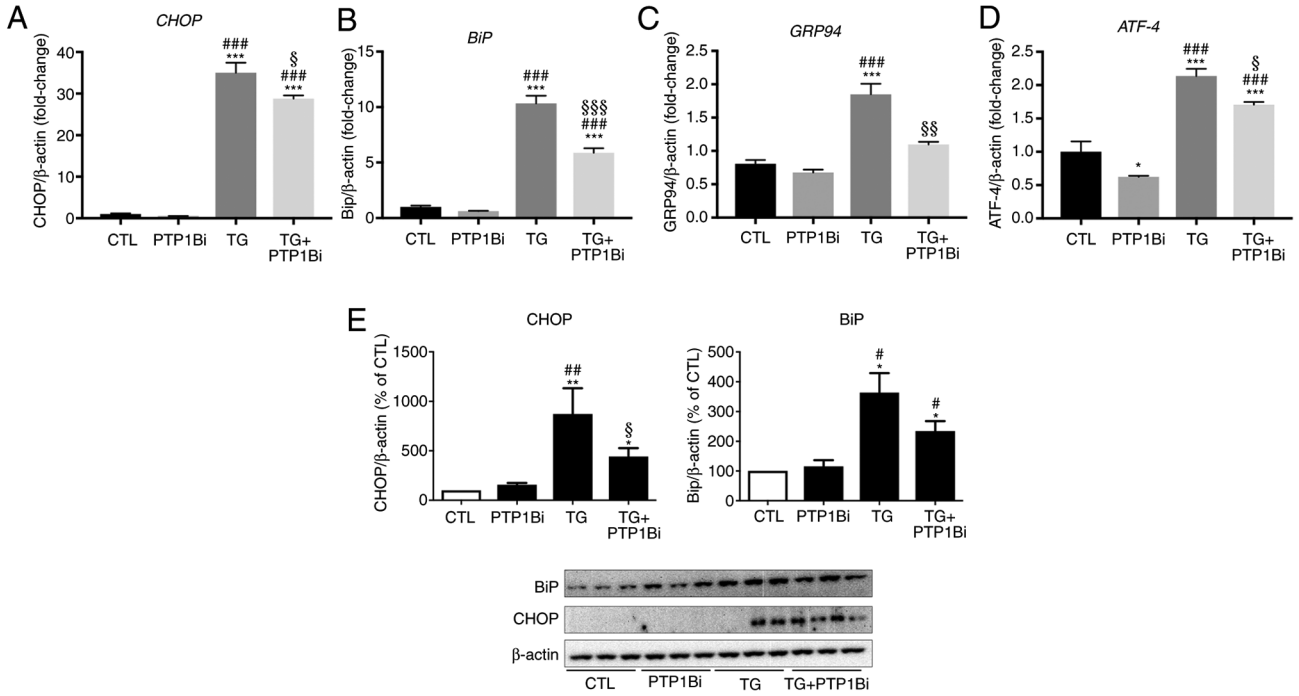

Figure 2. Impact of PTP1B inhibition on pharmacologically-induced endoplasmic reticulum stress in HUVECs. Reverse transcription-quantitative PCR analysis to assess mRNA expression of (A) *CHOP*, (B) *BiP*, (C) *GRP94* and (D) *ATF-4* and western blot analysis to assess protein expression levels of (E) CHOP and BiP in HUVECs exposed to TG (TG; 300 nM, 5 h) with or without PTP1Bi (BML, 20 μM, added 1 h prior to treatment). (A-D) mRNA expression was normalized against the housekeeping gene *β-actin* (n=6 in each group). (E) Bars represent the pooled densitometry data of protein expression of CHOP (left panel) and BiP (right panel) normalized to loading control β-actin and expressed as percentage (%) of untreated group (CTL) (n=4 in each group). All data are presented as the mean ± SEM. *P<0.05, **P<0.01, ***P<0.001 vs. CTL group; $^{\#}$P<0.05, $^{\#\#}$P<0.01, $^{\#\#\#}$P<0.001 vs. PTP1Bi group; §P<0.05, §§P<0.01 and §§§P<0.001 vs. TG group. PTP1B, protein tyrosine phosphatase 1B; HUVECs, human umbilical vein endothelial cells; BiP, endoplasmic reticulum resident chaperone immunoglobulin binding protein; GRP94, 94 kDa glucose-regulated protein; ATF-4, activating transcription factor 4; TG, thapsigargin; CTL, control; PTP1Bi, PTP1B inhibitor.

the mRNA expression levels of key inflammatory molecules was assessed in endothelial cells exposed to ER stressors. It was identified that the exposure of HUVECs to TG (300 nM; 5 h) caused a significant increase in the mRNA expression levels of *IL-6* (Fig. 4A), *IL-8* (Fig. 4B), *ICAM-1* (Fig. 4C) and *MCP-1* (Fig. 4D). In addition, PTP1B inhibition partially prevented this increase for all these molecules except *MCP-1* (Fig. 4A-D), showing a significant effect. Consistent with these observations, the treatment of EA.hy926 endothelial cells with DTT (2 mM; 24 h) also increased the mRNA expression levels of *IL-6* (Fig. 4E) and *IL-8* (Fig. 4F), which were both partially prevented in the presence of PTP1B inhibitor. These data demonstrated the protective effect of PTP1B inhibition against the ER stress-mediated increased in the mRNA expression levels of pro-inflammatory factors in endothelial cells.

Effect of PTP1B inhibition on the angiogenic capacity of endothelial cells subjected to ER stress. Another hallmark of endothelial function is the angiogenic capacity of endothelial cells, which is the capacity of endothelial cells to re-arrange themselves to create a tube-like structure on a 3-diemnsional matrix. This capacity is mainly regulated under the effects of VEGF-A activity (30). To study the impact of PTP1B inhibition on the angiogenic capacity of endothelial cells, HUVECs treated with TG with or without a PTP1B inhibitor were collected and seeded on top of a Matrigel matrix layer, then incubated for a further 4-6 h, allowing them time to form tube-like structures. It was demonstrated that TG significantly impaired the ability of the HUVECs to form tube-like structures (Fig. 5A), as evidenced by the reduction in the average length of tubes formed (Fig. 5B), indicating impairment in angiogenic capacity. The pre-treatment of cells with the PTP1B inhibitor prevented the deleterious effects of TG on tube-like structure formation (Fig. 5A and B).

Subsequently, the mRNA expression levels of various pro-angiogenic molecules were assessed. As presented in Fig. 5C, the treatment of cells with TG induced an upregulation in *VEGF-A* mRNA expression, while the pre-treatment of cells with a PTP1B inhibitor significantly reduced this effect. On the other hand, PTP1B inhibition did not affect the mRNA expression levels of fibroblast growth factor (*FGF*)-1 (Fig. 5D) and moderately increased those of *FGF-2* (Fig. 5E). Although the treatment of HUVECs with TG alone did not affect mRNA expression of *FGF-1* (Fig. 5D) and *FGF-2* (Fig. 5E) compared with the control group, the pre-treatment of cells with a PTP1B inhibitor enhanced the mRNA expression levels of both *FGF-1* and *FGF-2* in the presence of TG (Fig. 5D and E) compared with all other groups.

Effect of PTP1B inhibition and silencing on ER stress-mediated apoptosis. ER stress-induced apoptosis is a major contributor to the loss of endothelial cells, which predisposes individuals to strokes and cardiovascular complications (39). Therefore, the current study assessed the impact of PTP1B suppression on the survival of HUVECs exposed to pharmacological ER stress. As shown in Fig. 6A, cell cycle analysis

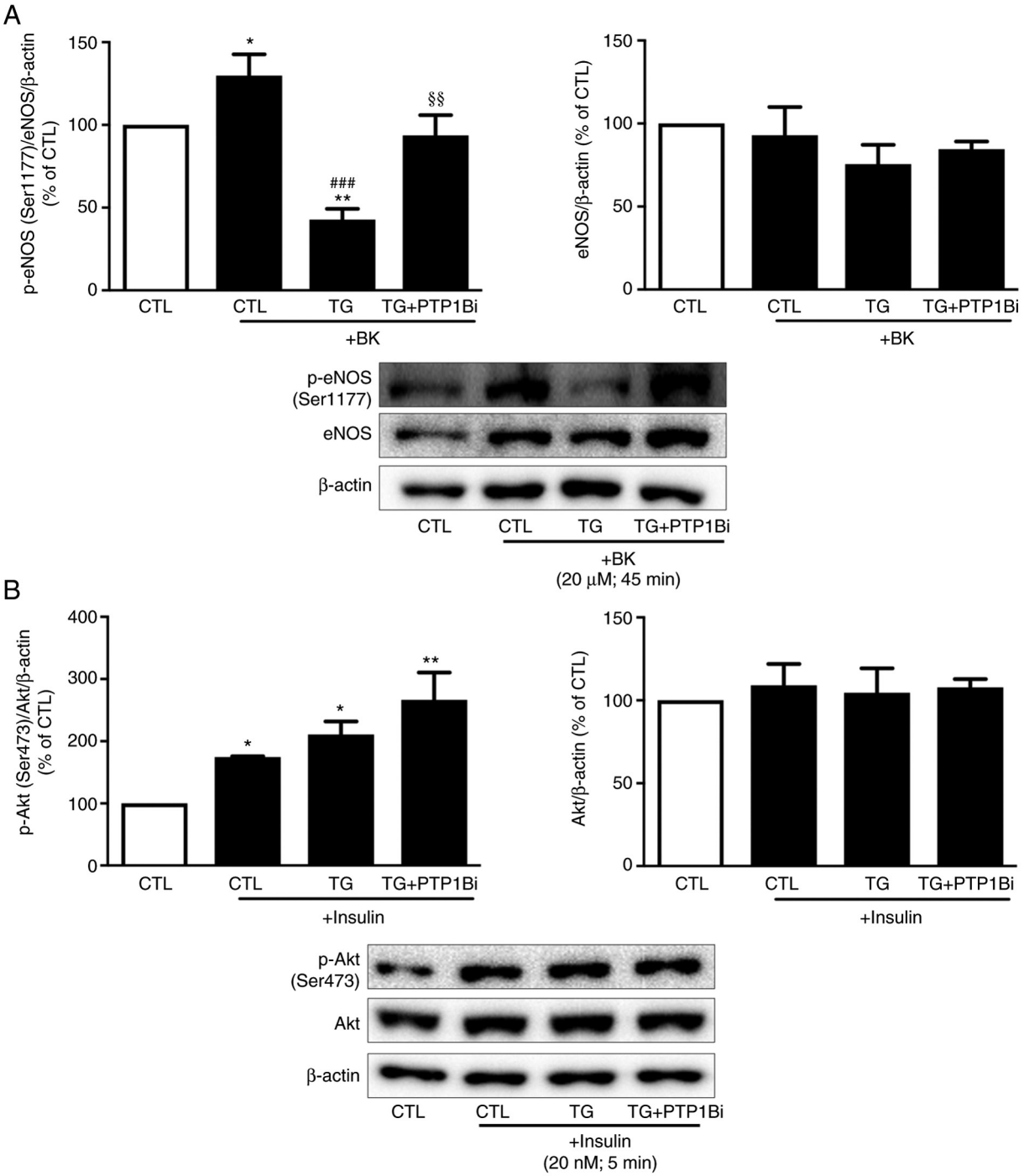

Figure 3. Impact of PTP1B inhibition on eNOS and Akt phosphorylation in HUVECs subjected to endoplasmic reticulum stress. Western blot analysis to assess protein expression levels of (A) p-eNOS (Ser1177) and total eNOS, and (B) p-Akt (Ser473) and total Akt in HUVECs treated with TG (300 nM for 5 h) in the presence or absence of PTP1Bi (BML, 20 μM, added 1 h prior to treatment), followed by the incubation of cells with either (A) BK (20 μM, 45 min) or (B) insulin (20 nM, 5 min). Left bars represent the pooled densitometry data of p-proteins normalized to respective total protein (eNOS or Akt) and to loading control β-actin. Right bars show pooled densitometry data of total proteins (eNOS or Akt) normalized to loading control β-actin. Data are expressed as percentage (%) of untreated group (CTL) (n=4 in each group). All data are presented as the mean ± SEM. *P<0.05, **P<0.01 vs. CTL group; $^{\#\#\#}$P<0.001 vs. CTL + BK group; §§P<0.01 vs. TG + BK group. PTP1B, protein tyrosine phosphatase 1B; HUVECs, human umbilical vein endothelial cells; eNOS, endothelial nitric oxide synthase; p-, phosphorylated; TG, thapsigargin; BK, bradykinin; CTL, control; PTP1Bi, PTP1B inhibitor.

revealed that TG-mediated ER stress induction resulted in cell cycle progression disruption, as evidenced by the increase in the percentage of cells in sub-G_1 phase (apoptotic cells) and a reduction in the proportion of cells in G_0/G_1 phase, in addition to the increase in the percentage of cells in G_2/M phase of the cycle, compared with both untreated cells and those pre-treated with PTP1B inhibitor alone. Of note, PTP1B inhibition prevented all the effects of ER stress activation on cell cycle progression (Fig. 6A).

Subsequently, the impact of PTP1B inhibition on the number of apoptotic cells following exposure to TG was investigated. The results demonstrated that TG caused a

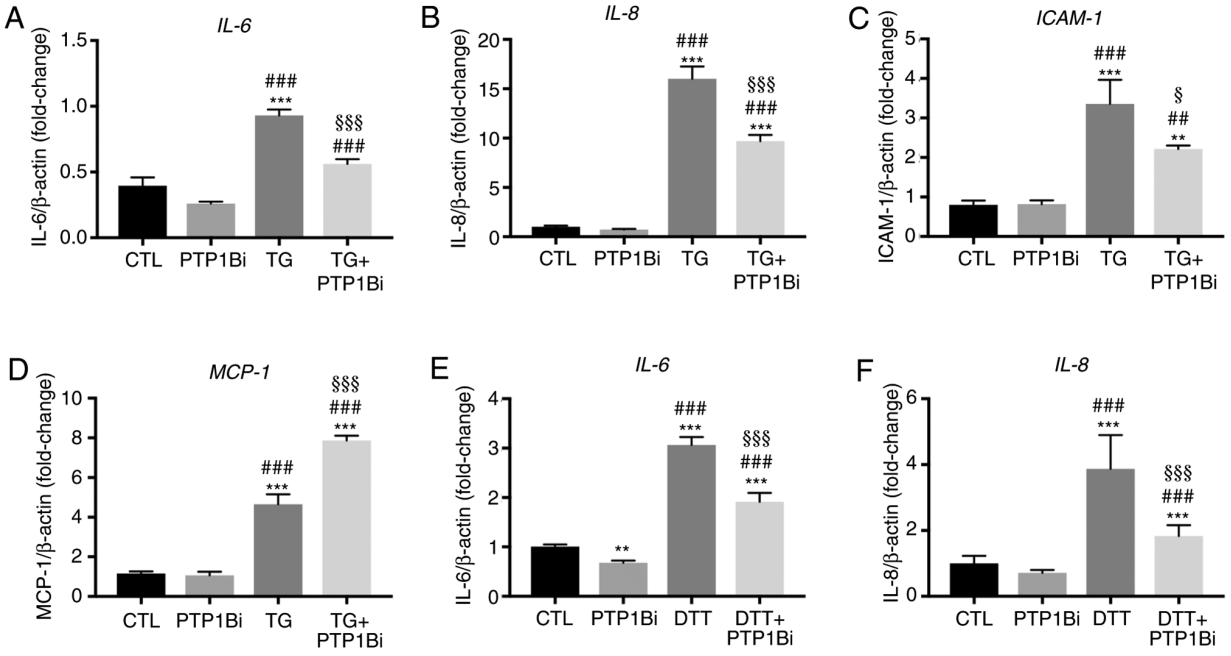

Figure 4. Impact of PTP1B inhibition on the mRNA expression levels of pro-inflammatory genes in endothelial cells subjected to endoplasmic reticulum stress. (A-D) Human umbilical vein endothelial cells were exposed to TG (300 nM, 5 h) with or without PTP1Bi (BML, 20 μM, added 1 h prior to treatment). Then, relative mRNA expression of (A) *IL-6*, (B) *IL-8*, (C) *ICAM-1* and (D) *MCP-1*, was determined and normalized against housekeeping gene β-actin (n=6 per group). (E and F) EA.hy926 cells were exposed to DTT (2 mM, 24 h) with or without PTP1Bi (BML, 20 μM, added 1 h prior to treatment). Then, relative mRNA expression of (E) *IL-6* and (F) *IL-8* was determined and normalized against housekeeping gene β-actin (n=6 per group). All data are presented as the mean ± SEM. **P<0.01, ***P<0.001 vs. CTL group; $^{\#\#}$P<0.01, $^{\#\#\#}$P<0.001 vs. PTP1Bi group; §P<0.05, §§§P<0.001 vs. TG group. PTP1B, protein tyrosine phosphatase 1B; ICAM-1, intracellular molecular adhesion-1; MCP-1, monocyte chemoattractant protein-1; TG, thapsigargin; DTT, 1,4-dithiothreitol; CTL, control; PTP1Bi, PTP1B inhibitor.

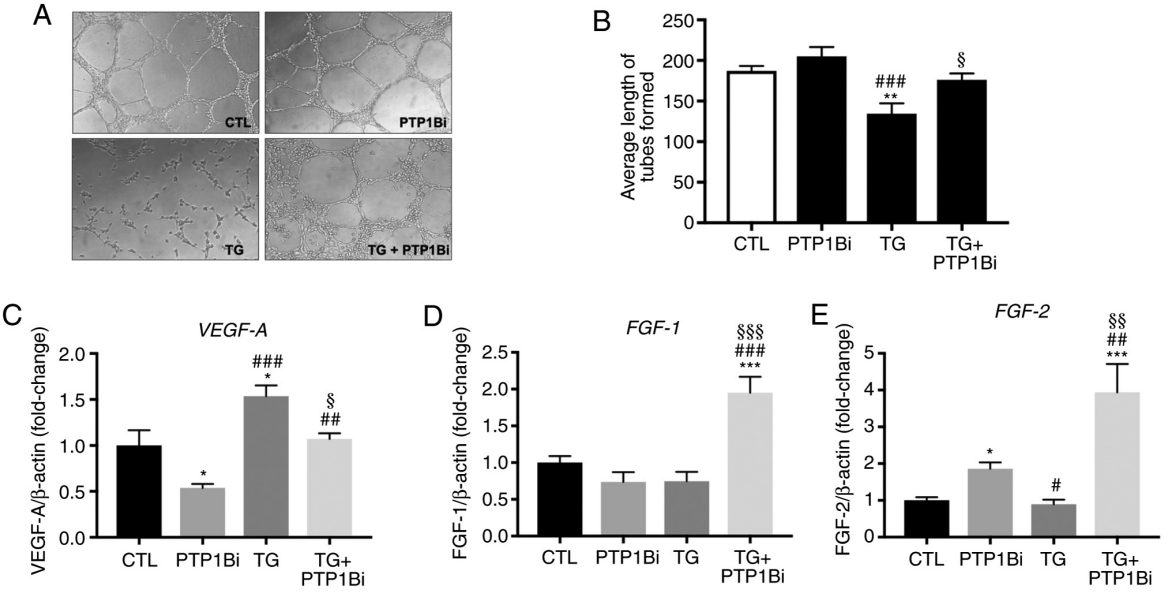

Figure 5. Impact of PTP1B inhibition on the angiogenic capacity of HUVECs subjected to pharmacological endoplasmic reticulum stress. (A) Matrigel-based tube formation assay of HUVECs treated with TG (TG; 300 nM, 5 h) with or without PTP1Bi (BML, 20 μM, added 1 h prior to treatment). Images are representative of three independent experiments. (B) Bars represent pooled data of the quantification of angiogenic capacity, expressed as the average length of tubes formed that were counted in five random fields for each well using WimTube software (n=3 per group). Relative mRNA expression of (C) *VEGF-A*, (D) *FGF-1* and (E) *FGF-2*, normalized against housekeeping gene β-actin (n=6 per group). All data are presented as the mean ± SEM. *P<0.05, **P<0.01, ***P<0.001 vs. CTL group; $^{\#}$P<0.05, $^{\#\#}$P<0.01, $^{\#\#\#}$P<0.001 vs. PTP1Bi group; §P<0.05, §§P<0.01, §§§P<0.001 vs. TG group. PTP1B, protein tyrosine phosphatase 1B; HUVECs, human umbilical vein endothelial cells; TG, thapsigargin; PTP1Bi, PTP1B inhibitor; FGF, fibroblast growth factor; CTL, control.

significant reduction in the number of live HUVECs, while at the same time increasing the number of dead and apoptotic cells (Fig. 6B). Moreover, the inhibition of PTP1B resulted in a marked decrease in the number of apoptotic cells, thus reducing the pro-apoptotic actions of TG (Fig. 6B). This finding indicated the beneficial role of PTP1B inhibition in reducing

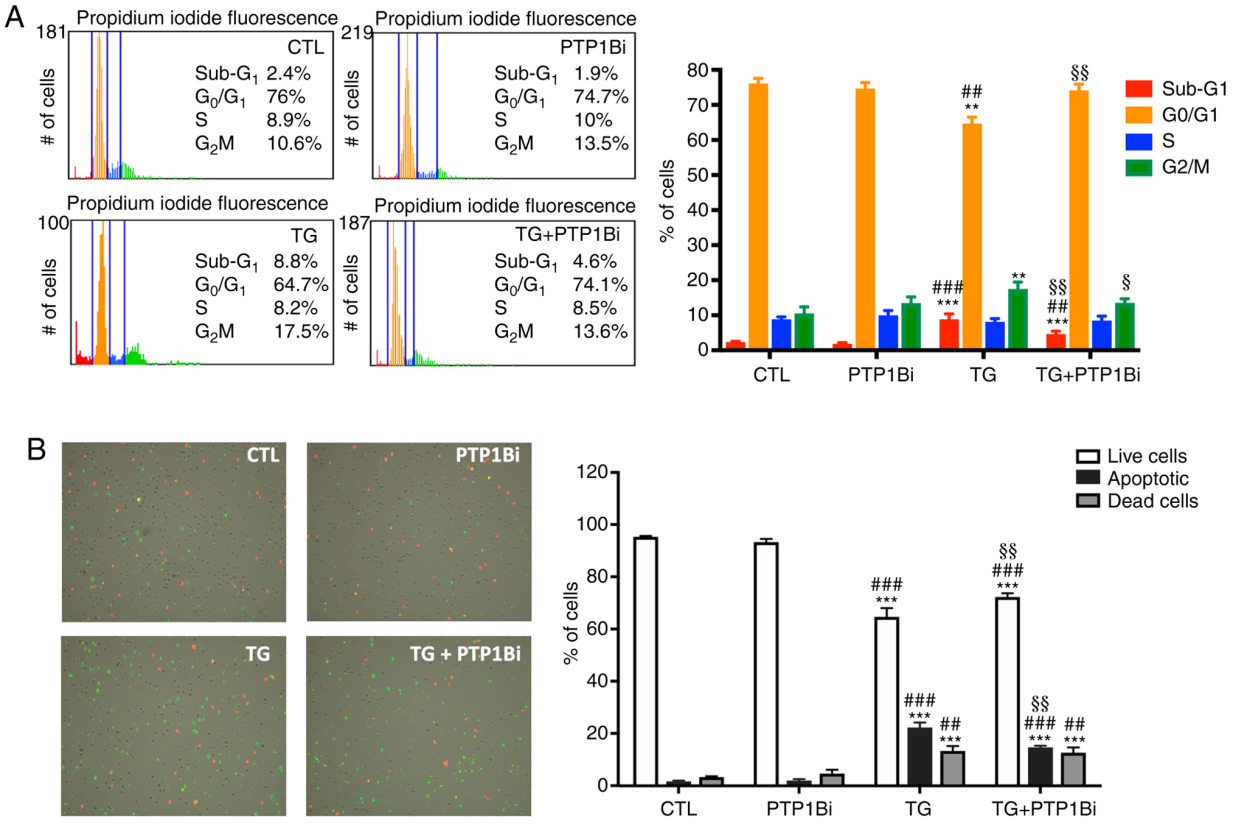

Figure 6. Impact of PTP1B inhibition on cell survival of HUVECs subjected to pharmacological endoplasmic reticulum stress. (A) Tali image-based cytometer analysis of cell cycle in HUVECs treated with TG (300 nM, 5 h) treated with or without PTP1Bi (BML, 20 μM, added 1 h prior to treatment) (n=4 in each group). Bars represent the percentages of cells in each phase of cell cycle: Sub-G_1 (apoptotic cells), G_0/G_1, S and G_2/M. Representative fluorescence images of cell cycle phases are shown: Red (Sub-G_1 or apoptotic), orange (G_0/G1), blue (S) and green (G_2/M). (B) Tali image-based cytometer analysis of apoptosis in HUVECs treated with TG (300 nM, 5 h) treated with or without PTP1Bi (BML, 20 μM, added 1 h prior to treatment) (n=4 in each group). Bars represent the percentages of live, apoptotic and dead cells. Representative fluorescence images are shown to indicate apoptotic cells in green color, dead cells in red and green (appear yellow), and live cells with little or no fluorescence. Average percentage of cells in each phase of the cell cycle is shown on each Tali representative fluorescence image of each experimental group. All data are presented as the mean ± SEM. **P<0.01, ***P<0.001 vs. CTL group; $^{\#\#}$P<0.01, $^{\#\#\#}$P<0.001 vs. PTP1Bi group; §P<0.05, §§P<0.01 vs. TG group. PTP1B, protein tyrosine phosphatase 1B; HUVECs, human umbilical vein endothelial cells; TG, thapsigargin; PTP1Bi, PTP1B inhibitor; CTL, control.

ER stress-mediated apoptosis. To further examine the role of PTP1B in this mechanism, instead of pharmacologically inhibiting PTP1B, its protein expression was knocked down using specific siRNA duplexes. As shown in Fig. 7A, the treatment of HUVECs with PTP1B siRNA duplexes significantly reduced PTP1B mRNA expression compared with untreated cells and those incubated with scrambled siRNA. HUVECs were incubated with or without PTP1B siRNA for 48 h to knockdown PTP1B protein expression, followed by incubation with or without TG. As presented in Fig. 7B, TG-induced ER stress caused a slight, but statistically significant, increase in PTP1B protein expression compared with the control group, which was not observed in the PTP1B knockdown groups. The exposure of HUVECs to TG caused the number of live cells to decrease significantly, while increasing the proportion of apoptotic cells (Fig. 7C), which was similar to what was observed with PTP1B inhibitor as depicted in Fig. 6B. This pro-apoptotic effect caused by TG was partially, but significantly prevented in endothelial cells subjected to PTP1B knockdown (Fig. 7C).

To investigate the role PTP1B serves in ER stress-mediated cell death, the protein expression levels of several apoptotic effectors were determined in HUVECs subjected to pharmacological ER stress with or without PTP1B inhibitor. While no changes in the protein expression levels of cleaved caspase-9 (Fig. 8A) and caspase-12 (Fig. 8B) were caused by TG, the pre-treatment of cells with a PTP1B inhibitor significantly reduced the expression level of caspase-12 (Fig. 8B) compared with the control or TG alone groups. Moreover, TG increased the protein expression level of cleaved PARP-1, while PTP1B inhibition prevented this effect (Fig. 8C).

As PTP1B inhibition was beneficial in reducing ER stress-mediated apoptosis, and hence, in promoting endothelial cell survival, the effect of PTP1B inhibition on ER stress-mediated autophagy, which serves a central role in cell survival (40), was also assessed. HUVECs were treated with TG with or without a PTP1B inhibitor, and then the protein expression levels of the autophagy marker LC3-II were determined. It was identified that TG significantly increased the expression level of LC3-II (Fig. 8D), indicating enhanced autophagy as a result of ER stress induction. Furthermore, PTP1B inhibition prevented this increased expression of the autophagy marker caused by TG (Fig. 8D), which may serve a key role in the improved survival of endothelial cells.

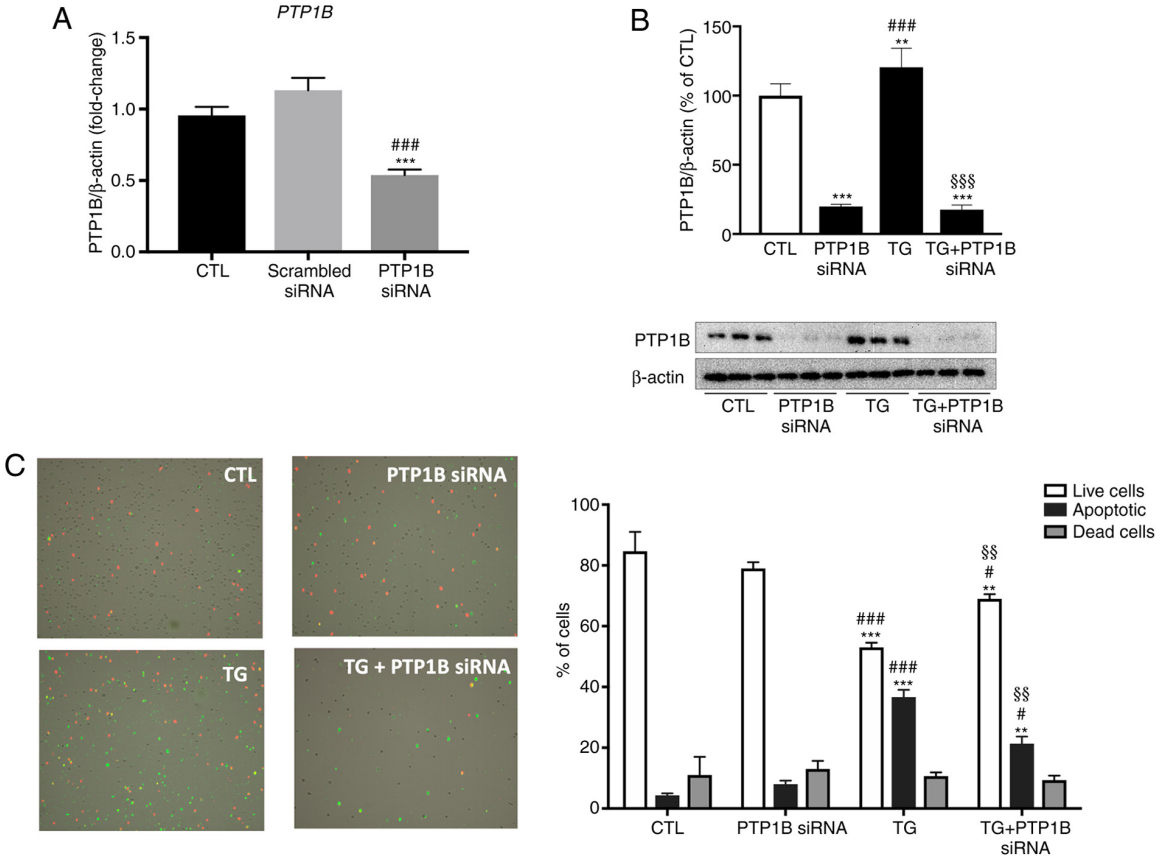

Figure 7. Impact of PTP1B silencing on apoptosis of HUVECs subjected to pharmacological endoplasmic reticulum stress. (A) Relative mRNA expression of *PTP1B* in untreated HUVECs and cells treated with either scrambled or *PTP1B* siRNA duplexes (15 nM for 72 h) normalized against housekeeping gene β-actin (n=6 per group). (B) Western blot analysis to assess protein expression levels of PTP1B in HUVECs incubated with or without *PTP1B* siRNA duplexes (15 nM for 72 h) in the presence or absence of TG (300 nM, 5 h). Bars represent the pooled densitometry data normalized to housekeeping protein β-actin and expressed as percentage (%) of untreated group (CTL) (n=4 in each group). (C) Tali image-based cytometer analysis for apoptosis of HUVECs treated with TG (300 nM, 5 h) with or without *PTP1B* siRNA duplexes (n=4 in each group). Bars represent the percentages of live, apoptotic and dead cells. Representative fluorescence images are shown to indicate apoptotic cells in green color, dead cells in red and green (appear yellow), and live cells with little or no fluorescence. All data are presented as the mean ± SEM. **P<0.01, ***P<0.001 vs. CTL group; $^{\#}$P<0.05, $^{\#\#\#}$P<0.001 vs. scrambled siRNA or PTP1B siRNA group; §§P<0.01, §§§P<0.001 vs. TG group. PTP1B, protein tyrosine phosphatase 1B; HUVECs, human umbilical vein endothelial cells; siRNA, small interfering RNA; TG, thapsigargin; CTL, control.

To further evaluate the implication of PTP1B in ER stress-mediated cell death, the impact of PTP1B inhibition on a major pro-proliferative signal, namely ERK1/2, was assessed. The results demonstrated that TG-induced ER stress impaired the phosphorylation of ERK1/2 (Fig. 8E), which may contribute to cell cycle arrest and apoptosis observed with TG administration. Surprisingly, the inhibition of PTP1B failed to correct this molecular alteration caused by TG (Fig. 8E).

Discussion

The present study aimed to investigate the molecular mechanisms underlying PTP1B-mediated endothelial dysfunction, by assessing the role of the crosstalk between PTP1B and ER stress in the development of endothelial dysfunction. The current study examined the benefits and impact of PTP1B silencing or inhibition on providing protection to endothelial cells against ER stress-mediated impairment of eNOS activation, insulin response, angiogenic capacity and, most importantly, ER stress-induced apoptosis, as well as determined the underlying pathways.

To the best of our knowledge, the present study reported for the first time that PTP1B inhibition protected HUVECs from ER stress-mediated impaired angiogenic capacity of endothelial cells. It was found that TG-induced ER stress abolished the ability of HUVECs to form capillary-like structures when incubated on a 3-dimentional extracellular Matrigel matrix. Moreover, PTP1B inhibition prevented the impairment caused by TG-induced ER stress and restored the angiogenic capacity of HUVECs. To obtain an improved understanding of the crosstalk between PTP1B and ER stress in the impairment of endothelial function, the current study investigated the impact of PTP1B blockade on the NO signaling pathway by determining at the levels of p-eNOS and p-Akt in HUVECs challenged with TG and stimulated with bradykinin and insulin, respectively. While ER stress induction by TG reduced bradykinin-stimulated phosphorylation of eNOS at the activator site (Ser1177), it did not affect the response of endothelial cells to insulin, as evident by the phosphorylation of Akt (Ser473). However, PTP1B inhibition partially restored the bradykinin-stimulated phosphorylation of eNOS at Ser1177 and enhanced insulin-stimulated Akt phosphorylation. In addition, PTP1B inhibition and deletion protected

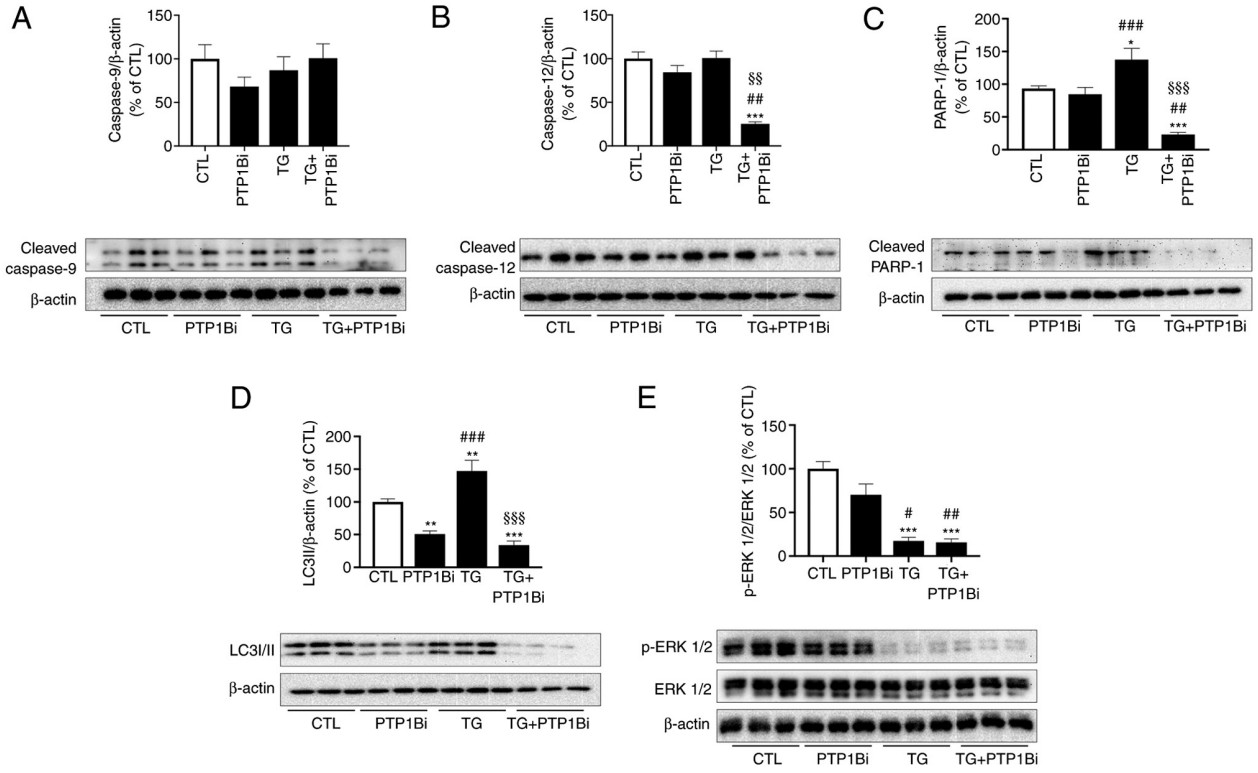

Figure 8. Impact of PTP1B inhibition on apoptotic signals in HUVECs subjected to pharmacological endoplasmic reticulum stress. Western blot analysis to assess protein expression levels of (A) cleaved caspase-9, (B) cleaved caspase-12, (C) cleaved PARP-1, (D) LC3I/II and (E) p-ERK 1/2 in HUVECs treated with TG (300 nM, 5 h) with or without PTP1Bi (BML, 20 μM, added 1 h prior to treatment). Bars represent the pooled densitometry data of protein expression normalized to respective total protein (ERK 1/2) or to loading control protein β-actin and expressed as percentage (%) of untreated group (CTL) (n=5 in each group). All data are presented as the mean ± SEM. *P<0.05, **P<0.01, ***P<0.001 vs. CTL group; $^{\#}$P<0.05, $^{\#\#}$P<0.01, $^{\#\#\#}$P<0.001 vs. PTP1Bi group; §§P<0.01, §§§P<0.001 vs. TG group. PTP1B, protein tyrosine phosphatase 1B; HUVECs, human umbilical vein endothelial cells; PARP-1, poly (ADP-ribose) polymerase-1; p-, phosphorylated; TG, thapsigargin; PTP1Bi, PTP1B inhibitor; CTL, control.

HUVECs against the pro-apoptotic effects of TG-induced ER stress, as demonstrated by the reduced number of apoptotic cells and blunted increase in the expression levels of key apoptotic effectors. Furthermore, one of the most important findings was that PTP1B inhibition protected endothelial cells against ER stress-induced autophagy without affecting other pro-apoptotic or proliferative signaling responses.

ER stress is implicated in a wide range of pathologies, such as diabetes, neurodegenerative disorders and, of particular interest, endothelial dysfunction. ER stress induction was confirmed by determining the expression levels of several ER stress markers. The present study observed a significant increase in the expression levels of *CHOP*, *BiP*, *ATF-4* and *GRP94*. These results were in line with those of Thiebaut *et al* (41) who reported an increase in the expression levels of p-eukaryotic initiation factor-2α, HSPA5 and ATF-6. However, in contrast to the current study, these authors reported no change in the expression of pro-apoptotic molecule CHOP. This discrepancy may be due to the use of different ER stress inducers (tunicamycin vs. DTT and TG in the present study). With regards to cell models used in this study, EA.hy926 are an immortalized cell line derived from HUVECs, while HUVECs, are primary endothelial cells and thus are more physiologically relevant. Initially, the present study determined the impact of PTP1B inhibition on ER stress response caused by both DTT and TG in immortalized (EA.hy926) and primary HUVECs cells. It was observed that PTP1B blockade reduced mRNA overexpression of pro-inflammatory molecules and ER stress markers caused by both DTT and TG. Therefore, for the rest of the study, TG was used as the ER stress inducer due to its strong response compared with DTT, and primary HUVECs were used as the cell model for functional experiments as they had higher physiological relevance compared with EA.hy926 cells.

ER stress activation is closely associated with cellular inflammation. Endothelial dysfunction precedes and imitates inflammatory response, where, at their surface, dysfunctional endothelial cells expose various adhesion molecules, such as ICAM-1, together with the release of multiple pro-inflammatory cytokines and chemokines, including IL-6, IL-8 and MCP-1 (42). The present study demonstrated that exposure of endothelial cells to TG enhanced the mRNA expression levels of *IL-6*, *IL-8*, *MCP-1,* and *ICAM-1*, while pre-treatment of cells with a PTP1B inhibitor significantly reduced the effects of TG on the mRNA expression levels of *IL-6*, *IL-8* and *ICAM-1*. The expression levels of adhesion molecules and the secretion of pro-inflammatory cytokines by activated endothelial cells can attract and facilitate the passage of monocytes through the vascular wall and promote a pro-inflammatory environment (43). In this context, PTP1B has been shown to be involved in the regulation of inflammatory responses (9,38). Moreover, specific deletion of PTP1B in mouse microphages has been revealed to protect animals from both obesity and lipopolysaccharide-mediated inflammatory response, where microphages collected from myeloid-PTP1B deficient mice

had lower levels of TNF-α and a higher expression of IL-10, an anti-inflammatory cytokine (44). It has also been reported that mice deficient for PTP1B specifically in microphages and deficient for apolipoprotein E (ApoE) in the whole body exhibited smaller atherosclerotic plaque size and higher plasma levels of IL-10 and prostaglandin E2, compared with ApoE-deficient mice only (45). In the current study, no animal studies were performed, which might be perceived as a limitation; however, the present findings are in line with our previous observations using *PTP1B* tissue-specific knockout animals (14,44).

A recent study investigated the ER stress-mediated endothelial dysfunction (46); however, this previous study only examined endothelium-dependent relaxation in response to acetylcholine, without assessing the impact on NO signaling or endothelial angiogenic capacity. NO is an important mediator and reflector of endothelial function (17). To study the impact of PTP1B inhibition on ER stress-mediated endothelial dysfunction, the present study assessed the impact of PTP1B deletion on NO signaling. Moreover, the phosphorylation levels eNOS and Akt in response to bradykinin and insulin, respectively, were evaluated in TG-challenged HUVECs. It was found that TG-induced ER stress resulted in reduced bradykinin-stimulated eNOS phosphorylation at Ser1177, while it did not affect the phosphorylation of Akt. Furthermore, PTP1B inhibition partially restored bradykinin-stimulated eNOS phosphorylation and enhanced the phosphorylation of Akt, showing a significant effect. The present results are in line with the effects observed in human aortic endothelial cells challenged with palmitate, a saturated free fatty acid known to induce ER stress, which resulted in a reduction in eNOS and Akt phosphorylation, which were restored by tauroursodeoxycholic acid, a chemical chaperone known to alleviate the ER stress response (47). However, in disagreement with the current study, in this previous study ER stress induction reduced Akt phosphorylation in response to insulin (47). One possible reason for this difference is the different cell line used, human aortic endothelial cells compared with HUVECs in the current report. Another reason for discrepancy could be the use of different ER stress inducers, palmitate-induced Toll-like receptor 4 in the study by Kim *et al* (47) compared with the use of TG in the present study. While the current data suggested that eNOS may be targeted by PTP1B, with our current experimental setting, it is difficult to assess the exact relationship between them. On the one hand, eNOS has been shown to be phosphorylated at tyrosine residues (48), which makes it a plausible target for dephosphorylation by PTP1B; however, answering this may require additional investigation, such as a phospho-proteomic approach, since the targeting of tyrosine residues is yet to be fully elucidated. Furthermore, eNOS has a complex role in endothelial dysfunction as its expression and phosphorylation are not the only regulators of its function since eNOS can also be uncoupled and instead of producing NO, it can start producing superoxide radicals under certain stress conditions (49).

The current study also assessed the angiogenic capacity of endothelial cells, where it was found that TG-induced ER stress markedly impaired the angiogenic ability of HUVECs. This was in accordance with other studies that revealed that ER stress induction impairs angiogenesis (1,30,50). A previous study revealed that the isolated aorta from rats exposed to TG displayed a significant inhibition in micro-vessel formation compared with controls. In the same study, the proliferation and migration of HUVECs were also impaired by TG-induced ER stress (50). Our previous study reported that exposure of HUVECs to TG impaired angiogenic capacity via a mechanism involving oxidative stress, and that this effect was prevented by 4-Phenylbutyric (PBA), a chemical chaperone that improves ER homeostasis (24). Moreover, the present study identified that PTP1B inhibition in HUVECs prevented the impairment of angiogenic capacity caused by TG and restored the tube-like formation ability of endothelial cells. This finding was in accordance with a study by Zhang *et al* (51), who showed that the treatment of human microvascular endothelial cells with high glucose (30 mM) for 12 h, followed by overlaying the cells on a Matrigel-coated dish, resulted in an impairment in tube formation capacity. Furthermore, this effect was largely prevented by PTP1B inhibition (51). The present study examined the mRNA expression levels of the pro-angiogenic factors *VEGF-A*, *FGF-1* and *FGF-2*, and it was observed that TG treatment caused a decrease in the expression level of *VEGF-A*, while PTP1B blockade prevented this. In addition, an increase in the mRNA expression levels of *FGF-1* and *FGF-2* was observed in cells challenged with TG in the presence of a PTP1B inhibitor, compared with control cells. The increase in *VEGF-A* mRNA expression in the TG group may be a compensatory mechanism to the impaired angiogenic response. PTP1B has been shown to negatively regulate VEGFR rather than affecting the expression level of VEGF (52). Overexpression of PTP1B was reported to decrease the phosphorylation of both VEGFR2 and Akt in bovine aortic endothelial cells following exposure to VEGF; however, the silencing of PTP1B enhanced the phosphorylation of these targets (52). Furthermore, the genetic deficiency of PTP1B was found to improve the angiogenic response in hearts from a mouse model of myocardial infarction via a mechanism involving improved VEGFR2 signaling (53).

The UPR response initially aims at restoring ER homeostasis and alleviating cellular stress; however, the sustained activation of UPR leads to ER stress and shifts the response from survival to apoptosis and cell death (1,17). Thus, the present study examined the impact of PTP1B inhibition and silencing on preventing ER stress-mediated endothelial cell death. As expected, HUVECs treated with TG displayed a significantly high percentage of apoptotic cells. This was in line with our previous observations in HUVECs exposed to TG (30) and findings by Huang *et al* (31), which revealed that vascular endothelial cells exposed to TG had an increased rate of cell apoptosis (31). The present study also demonstrated that both PTP1B deletion and inhibition reduced the proportion of apoptotic cells, thereby protecting the cells from the pro-apoptotic effects of TG. Similarly to the current observations, PTP1B inhibition was reported to protect cells against apoptosis in a human neuroblastoma cell line exposed to tunicamycin (54). In addition, mouse embryonic fibroblasts isolated from whole-body PTP1B deficient mice were observed to be resistant to tunicamycin-induced ER stress-mediated apoptosis (55). To further determine the apoptotic sub-pathways involved in this process, the current study assessed protein expression levels of several apoptotic effectors, including cleaved caspase-9, caspase-12 (specific

to ER stress) and PARP-1. An increasing trend in the expression levels of these effectors was observed in response to TG-induced ER stress. Similar results have been obtained in vascular endothelial cells treated with TG, where an increase in the expression levels of cleaved caspase-9 and -12 and PARP-1 was observed (31). Furthermore, we have previously observed that treatment of HUVECs with TG caused an increase in the expression of cleaved PARP-1, and executioner caspase-3 and caspase-7, which was prevented in cells pretreated with ER stress inhibitor, the chemical chaperone PBA (30). A similar pattern was observed in cells treated with high glucose, which also enhanced the enzymatic activity of caspase-3 and -7 (30).

There is a complex, tightly controlled and two-way relationship between MAPK and ER stress response (56,57). The present study demonstrated that TG reduced the activation of ERK 1/2. In general, the activation of the ERK 1/2 pathway is considered to encourage cell survival (56,57). Therefore, the reduction in the activation of ERK 1/2 caused by TG may contribute to cell growth arrest and reduced survival of endothelial cells. In the present study, the molecular alterations observed in the phosphorylation of ERK 1/2 were not prevented in the presence of the PTP1B inhibitor. This may suggest that the protective effects of PTP1B inhibition against ER stress-mediated apoptosis may be mediated via other signaling pathways, such as enhanced eNOS activity and the PI3K/Akt pro-survival pathway, a reduced autophagic response and a reduced expression of pro-inflammatory molecules, in addition to a possible enhancement in the insulin response in endothelial cells.

Autophagy is a crucial physiological process aiming to maintain a healthy cellular environment and homeostasis. However, excessive activation of autophagy results in cell death and has been associated with the pathogenesis of several cardiovascular diseases (40). The present study demonstrated that PTP1B inhibition protected endothelial cells from ER stress-mediated autophagy, as evidenced by reduced expression of its marker (LC3-II). The current study identified the excessive activation of autophagy in response to ER stress induction by TG and found that PTP1B inhibition completely prevented the activation of autophagy. These results are in line with those of Wang *et al* (58), who revealed that induction of ER stress *in vivo* via an injection of tunicamycin into mice resulted in the upregulation of LC3-II expression, which was significantly attenuated by genetic PTP1B deletion (58).

In conclusion, the present study provided evidence on the critical role of PTP1B in ER stress-mediated endothelial dysfunction, which was characterized by reduced angiogenic capacity via a mechanism involving reduced eNOS activation and cell survival. These findings demonstrated the therapeutic potential of targeting PTP1B in cardiovascular ischemic conditions.

Acknowledgements

Not applicable.

Funding

This work was supported by Qatar University grant (grant. no. QUCG-CPH-20/21-3) and awards from Qatar National Research Fund (a member of Qatar Foundation; grant. nos. NPRP-8-1750-3-360 and UREP24-016-3-004). SSA is supported by a graduate assistantship from the office of graduate studies (Qatar University).

Availability of data and materials

The datasets used and/or analyzed during the current study are available from the corresponding author on reasonable request.

Authors' contributions

AA conceptualized the present study, designed the research plan, and acquired resources and funding. AA supervised the experiments and collected the data. SSA, MP, HEG and MH performed the experiments and collected data. AA, SSA, MP, MAE, AZ and HMK performed formal data analysis. AA and SSA wrote the manuscript and prepared the figures with editing and input from all authors. MAE, AZ and HMK revised the manuscript critically for important intellectual content. AA and SSA confirm the authenticity of all the raw data. All authors have read and approved the final manuscript.

Ethics approval and consent to participate

Not applicable.

Patient consent for publication

Not applicable.

Competing interests

The authors declare that they have no competing interests.

References

1. Maamoun H, Benameur T, Pintus G, Munusamy S and Agouni A: Crosstalk between oxidative stress and endoplasmic reticulum (ER) stress in endothelial dysfunction and aberrant angiogenesis associated with diabetes: A focus on the protective roles of heme oxygenase (HO)-1. Front Physiol 10: 70, 2019.
2. Zhang HN, Xu QQ, Thakur A, Alfred MO, Chakraborty M, Ghosh A and Yu XB: Endothelial dysfunction in diabetes and hypertension: Role of microRNAs and long non-coding RNAs. Life Sci 213: 258-268, 2018.
3. Cersosimo E and DeFronzo RA: Insulin resistance and endothelial dysfunction: The road map to cardiovascular diseases. Diabetes Metab Res Rev 22: 423-436, 2006.
4. Potenza MA, Gagliardi S, Nacci C, Carratu MR and Montagnani M: Endothelial dysfunction in diabetes: From mechanisms to therapeutic targets. Curr Med Chem 16: 94-112, 2009.
5. Muniyappa R, Iantorno M and Quon MJ: An integrated view of insulin resistance and endothelial dysfunction. Endocrinol Metab Clin North Am 37: 685-711, 2008.
6. Bakke J and Haj FG: Protein-tyrosine phosphatase 1B substrates and metabolic regulation. Semin Cell Dev Biol 37: 58-65, 2015.
7. Tonks NK, Diltz CD and Fischer EH: Purification of the major protein-tyrosine-phosphatases of human placenta. J Biol Chem 263: 6722-6730, 1988.
8. Galic S, Klingler-Hoffmann M, Fodero-Tavoletti MT, Puryer MA, Meng TC, Tonks NK and Tiganis T: Regulation of insulin receptor signaling by the protein tyrosine phosphatase TCPTP. Mol Cell Biol 23: 2096-2108, 2003.

9. Abdelsalam SS, Korashy HM, Zeidan A and Agouni A: The role of protein tyrosine phosphatase (PTP)-1B in cardiovascular disease and its interplay with insulin resistance. Biomolecules 9: 286, 2019.
10. Vercauteren M, Remy E, Devaux C, Dautreaux B, Henry JP, Bauer F, Mulder P, van Huijsduijnen RH, Bombrun A, Thuillez C and Richard V: Improvement of peripheral endothelial dysfunction by protein tyrosine phosphatase inhibitors in heart failure. Circulation 114: 2498-2507, 2006.
11. Gomez E, Vercauteren M, Kurtz B, Ouvrard-Pascaud A, Mulder P, Henry JP, Besnier M, Waget A, Van Huijsduijnen RH, Tremblay ML, *et al*: Reduction of heart failure by pharmacological inhibition or gene deletion of protein tyrosine phosphatase 1B. J Mol Cell Cardiol 52: 1257-1264, 2012.
12. Agouni A, Tual-Chalot S, Chalopin M, Duluc L, Mody N, Martinez MC, Andriantsitohaina R and Delibegović M: Hepatic protein tyrosine phosphatase 1B (PTP1B) deficiency protects against obesity-induced endothelial dysfunction. Biochem Pharmacol 92: 607-617, 2014.
13. Gogiraju R, Schroeter MR, Bochenek ML, Hubert A, Münzel T, Hasenfuss G and Schäfer K: Endothelial deletion of protein tyrosine phosphatase-1B protects against pressure overload-induced heart failure in mice. Cardiovasc Res 111: 204-216, 2016.
14. Agouni A, Mody N, Owen C, Czopek A, Zimmer D, Bentires-Alj M, Bence KK and Delibegović M: Liver-specific deletion of protein tyrosine phosphatase (PTP) 1B improves obesity-and pharmacologically-induced endoplasmic reticulum stress. Biochem J 438: 369-378, 2011.
15. Owen C, Lees EK, Grant L, Zimmer DJ, Mody N, Bence KK and Delibegović M: Inducible liver-specific knockdown of protein tyrosine phosphatase 1B improves glucose and lipid homeostasis in adult mice. Diabetologia 56: 2286-2296, 2013.
16. Villalobos-Labra R, Subiabre M, Toledo F, Pardo F and Sobrevia L: Endoplasmic reticulum stress and development of insulin resistance in adipose, skeletal, liver, and foetoplacental tissue in diabesity. Mol Aspects Med 66: 49-61, 2018.
17. Maamoun H, Abdelsalam SS, Zeidan A, Korashy HM and Agouni A: Endoplasmic reticulum stress: A critical molecular driver of endothelial dysfunction and cardiovascular disturbances associated with diabetes. Int J Mol Sci 20: 1658, 2019.
18. Flamment M, Hajduch E, Ferré P and Foufelle F: New insights into ER stress-induced insulin resistance. Trends Endocrinol Metab 23: 381-390, 2012.
19. Özcan U, Cao Q, Yilmaz E, Lee AH, Iwakoshi NN, Ozdelen E, Tuncman G, Görgün C, Glimcher LH and Hotamisligil GS: Endoplasmic reticulum stress links obesity, insulin action, and type 2 diabetes. Science 306: 457-461, 2004.
20. Özcan U, Yilmaz E, Özcan L, Furuhashi M, Vaillancourt E, Smith RO, Görgün CZ and Hotamisligil GS: Chemical chaperones reduce ER stress and restore glucose homeostasis in a mouse model of type 2 diabetes. Science 313: 1137-1140, 2006.
21. Kassan M, Galán M, Partyka M, Saifudeen Z, Henrion D, Trebak M and Matrougui K: Endoplasmic reticulum stress is involved in cardiac damage and vascular endothelial dysfunction in hypertensive mice. Arterioscler Thromb Vasc Biol 32: 1652-1661, 2012.
22. Galán M, Kassan M, Choi SK, Partyka M, Trebak M, Henrion D and Matrougui K: A novel role for epidermal growth factor receptor tyrosine kinase and its downstream endoplasmic reticulum stress in cardiac damage and microvascular dysfunction in type 1 diabetes mellitus. Hypertension 60: 71-80, 2012.
23. Ghemrawi R, Battaglia-Hsu SF and Arnold C: Endoplasmic reticulum stress in metabolic disorders. Cells 7: 63, 2018.
24. Schwarz DS and Blower MD: The endoplasmic reticulum: Structure, function and response to cellular signaling. Cell Mol Life Sci 73: 79-94, 2016.
25. Pandey VK, Mathur A and Kakkar P: Emerging role of unfolded protein response (UPR) mediated proteotoxic apoptosis in diabetes. Life Sci 216: 246-258, 2019.
26. Battson ML, Lee DM and Gentile CL: Endoplasmic reticulum stress and the development of endothelial dysfunction. Am J Physiol Heart Circul Physiol 312: H355-H367, 2017.
27. Minamino T, Komuro I and Kitakaze M: Endoplasmic reticulum stress as a therapeutic target in cardiovascular disease. Circ Res 107: 1071-1082, 2010.
28. Bilekova S, Sachs S and Lickert H: Pharmacological targeting of endoplasmic reticulum stress in pancreatic beta cells. Trends Pharmacol Sci 42: 85-95, 2020.
29. Zeng L, Zampetaki A, Margariti A, Pepe AE, Alam S, Martin D, Xiao Q, Wang W, Jin ZG, Cockerill G, *et al*: Sustained activation of XBP1 splicing leads to endothelial apoptosis and atherosclerosis development in response to disturbed flow. Proc Natl Acad Sci USA 106: 8326-8331, 2009.
30. Maamoun H, Zachariah M, McVey JH, Green FR and Agouni A: Heme oxygenase (HO)-1 induction prevents Endoplasmic Reticulum stress-mediated endothelial cell death and impaired angiogenic capacity. Biochem Pharmacol 127: 46-59, 2017.
31. Huang J, Wan L, Lu H and Li X: High expression of active ATF6 aggravates endoplasmic reticulum stress-induced vascular endothelial cell apoptosis through the mitochondrial apoptotic pathway. Mol Med Rep 17: 6483-6489, 2018.
32. Choy JC, Granville DJ, Hunt DW and McManus BM: Endothelial cell apoptosis: Biochemical characteristics and potential implications for atherosclerosis. J Mol Cell Cardiol 33: 1673-1690, 2001.
33. Osman A, El-Gamal H, Pasha M, Zeidan A, Korashy HM, Abdelsalam SS, Hasan M, Benameur T and Agouni A: Endoplasmic reticulum (ER) stress-generated extracellular vesicles (Microparticles) self-perpetuate ER stress and mediate endothelial cell dysfunction independently of cell survival. Front Cardiovasc Med 7: 584791, 2020.
34. Abdullahi A, Stanojcic M, Parousis A, Patsouris D and Jeschke MG: Modeling acute ER stress in vivo and in vitro. Shock 47: 506-513, 2017.
35. Andersen HS, Olsen OH, Iversen LF, Sørensen AL, Mortensen SB, Christensen MS, Branner S, Hansen TK, Lau JF, Jeppesen L, *et al*: Discovery and SAR of a novel selective and orally bioavailable nonpeptide classical competitive inhibitor class of protein-tyrosine phosphatase 1B. J Med Chem 45: 4443-4459, 2002.
36. Agouni A, Mostefai HA, Porro C, Carusio N, Favre J, Richard V, Henrion D, Martínez MC and Andriantsitohaina R: Sonic hedgehog carried by microparticles corrects endothelial injury through nitric oxide release. FASEB J 21: 2735-2741, 2007.
37. Livak KJ and Schmittgen TD: Analysis of relative gene expression data using real-time quantitative PCR and the 2(-Delta Delta C(T)) method. Methods 25: 402-408, 2001.
38. Coquerel D, Neviere R, Delile E, Mulder P, Marechal X, Montaigne D, Renet S, Remy-Jouet I, Gomez E, Henry JP, *et al*: Gene deletion of protein tyrosine phosphatase 1B protects against sepsis-induced cardiovascular dysfunction and mortality. Arterioscler Thromb Vasc Biol 34: 1032-1044, 2014.
39. Wang Y, Fan Y, Song Y, Han X, Fu M, Wang J, Cui X, Cao J, Chen L, Hu K, *et al*: Angiotensin II induces apoptosis of cardiac microvascular endothelial cells via regulating PTP1B/PI3K/Akt pathway. In vitro Cell Dev Biol Animal 55: 801-811, 2019.
40. Lavandero S, Chiong M, Rothermel BA and Hill JA: Autophagy in cardiovascular biology. J Clin Invest 125: 55-64, 2015.
41. Thiebaut PA, Delile E, Coquerel D, Brunel JM, Renet S, Tamion F and Richard V: Protein tyrosine phosphatase 1B regulates endothelial endoplasmic reticulum stress; role in endothelial dysfunction. Vascul Pharmacol 109: 36-44, 2018.
42. Sun HJ, Wu ZY, Nie XW and Bian JS: Role of endothelial dysfunction in cardiovascular diseases: The link between inflammation and hydrogen sulfide. Front Pharmacol 21: 1568, 2020.
43. Lubrano V and Balzan S: Roles of LOX-1 in microvascular dysfunction. Microvasc Res 105: 132-140, 2016.
44. Grant L, Shearer KD, Czopek A, Lees EK, Owen C, Agouni A, Workman J, Martin-Granados C, Forrester JV, Wilson HM, *et al*: Myeloid-cell protein tyrosine phosphatase-1B deficiency in mice protects against high-fat diet and lipopolysaccharide-induced inflammation, hyperinsulinemia, and endotoxemia through an IL-10 STAT3-dependent mechanism. Diabetes 63: 456-470, 2014.
45. Thompson D, Morrice N, Grant L, Sommer SL, Ziegler K, Whitfield P, Mody N, Wilson HM and Delibegović M: Myeloid protein tyrosine phosphatase 1B (PTP1B) deficiency protects against atherosclerotic plaque formation in the ApoE$^{(-/-)}$ mouse model of atherosclerosis with alterations in IL10/AMPKα pathway. Mol Metab 6: 845-853, 2017.
46. Legeay S, Fautrat P, Norman JB, Antonova G, Kennard S, Bruder-Nascimento T, Patel VS, Faure S and de Chantemèle EJ: Selective deficiency in endothelial PTP1B protects from diabetes and endoplasmic reticulum stress-associated endothelial dysfunction via preventing endothelial cell apoptosis. Biomed Pharmacother 127: 110200, 2020.
47. Kim JA, Jang HJ and Hwang DH: Toll-like receptor 4-induced endoplasmic reticulum stress contributes to impairment of vasodilator action of insulin. Am J Physiol Endocrinol Metab 309: E767-E776, 2015.

48. Dixit M, Loot AE, Mohamed A, Fisslthaler B, Boulanger CM, Ceacareanu B, Hassid A, Busse R and Fleming I: Gab1, SHP2, and protein kinase A are crucial for the activation of the endothelial NO synthase by fluid shear stress. Circ Res 97: 1236-1244, 2005.
49. Karbach S, Wenzel P, Waisman A, Munzel T and Daiber A: eNOS uncoupling in cardiovascular diseases-the role of oxidative stress and inflammation. Curr Pharm Des 20: 3579-3594, 2014.
50. Shukla N, Freeman N, Gadsdon P, Angelini GD and Jeremy JY: Thapsigargin inhibits angiogenesis in the rat isolated aorta: Studies on the role of intracellular calcium pools. Cardiovasc Res 49: 681-689, 2001.
51. Zhang J, Li L, Li J, Liu Y, Zhang CY, Zhang Y and Zen K: Protein tyrosine phosphatase 1B impairs diabetic wound healing through vascular endothelial growth factor receptor 2 dephosphorylation. Arterioscler Thromb Vasc Biol 35: 163-174, 2015.
52. Zhang Y, Li Q, Youn JY and Cai H: Protein phosphotyrosine phosphatase 1B (PTP1B) in calpain-dependent feedback regulation of vascular endothelial growth factor receptor (VEGFR2) in endothelial cells: Implications in VEGF-dependent angiogenesis and diabetic wound healing. J Biol Chem 292: 407-416, 2017.
53. Besnier M, Galaup A, Nicol L, Henry JP, Coquerel D, Gueret A, Mulder P, Brakenhielm E, Thuillez C, Germain S, *et al*: Enhanced angiogenesis and increased cardiac perfusion after myocardial infarction in protein tyrosine phosphatase 1B-deficient mice. FASEB J 28: 3351-3361, 2014.
54. Jeon YM, Lee S, Kim S, Kwon Y, Kim K, Chung CG, Lee S, Lee SB and Kim HJ: Neuroprotective effects of protein tyrosine phosphatase 1B inhibition against ER stress-induced toxicity. Mol Cells 40: 280-290, 2017.
55. Gu F, Nguyên DT, Stuible M, Dubé N, Tremblay ML and Chevet E: Protein-tyrosine phosphatase 1B potentiates IRE1 signaling during endoplasmic reticulum stress. J Biol Chem 279: 49689-49693, 2004.
56. Hotamisligil GS and Davis RJ: Cell signaling and stress responses. Cold Spring Harb Perspect Biol 8: a006072, 2016.
57. Darling NJ and Cook SJ: The role of MAPK signalling pathways in the response to endoplasmic reticulum stress. Biochim Biophys Acta 1843: 2150-2163, 2014.
58. Wang S, Chen X, Nair S, Sun D, Wang X and Ren J: Deletion of protein tyrosine phosphatase 1B obliterates endoplasmic reticulum stress-induced myocardial dysfunction through regulation of autophagy. Biochim Biophys Acta Mol Basis Dis 1863: 3060-3074, 2017.